Indian Journal of Experimental Biology
Vol. 63, June 2025, pp. 482-490
DOI: 10.56042/ijeb.v63i06.14452

Antibacterial effect of silver and copper nanoparticles derived from *Klebsiella pneumoniae*-NSB2 strain against pathogenic bacteria

Kunal Madhav[1]*, Archana Pandita[1] & Diksha Rani[2]

[1]Department of Biotechnology, Sharda School of Engineering and Technology, Sharda University, Greater Noida, India

[2]Department of Microbiology, All India Institute of Medical Sciences, Rishikesh, India

Received 17 October 2024; revised 05 March 2025

The rising threat of multidrug-resistant (MDR) bacteria has escalated the search for alternative antimicrobial solutions, including the use of nanoparticles. This study evaluated antibacterial activity of biosynthesized silver (AgNP) and copper nanoparticles (CuNP), produced by the *Klebsiella pneumoniae* NSB-2 strain against *Escherichia coli* and *Staphylococcus aureus*. UV-Visible spectrophotometry confirmed the synthesis of these nanoparticles, with absorption peaks at 421 nm for AgNPs and 419 nm for CuNPs. TEM analysis revealed spherical nanoparticles with sizes of 29.3 nm for AgNPs and 31.5 nm for CuNPs. AgNPs demonstrated a minimum inhibitory concentration (MIC) of 30 µg/mL for both pathogens, while CuNPs had an MIC of 40 µg/mL for *E. coli* and 30 µg/mL for *S. aureus*. Both nanoparticles exhibited bactericidal activity at 40 µg/mL, with AgNPs showing greater antibacterial potency. Growth rate (µ) and doubling time (T_d) analyses revealed that bacterial growth slowed, and doubling times increased in the presence of both nanoparticles. Results indicate that AgNPs were more effective at lower concentrations compared to CuNPs, underscoring their stronger impact on bacterial growth kinetics. This study suggests that AgNPs and CuNPs hold promise as alternative treatments for MDR bacterial infections, with AgNPs showing superior efficacy.

Keywords: Nanomedicine, Specific growth rate, Doubling time, MDR, Bacterial growth kinetics

Emergence of multi-drug resistant bacteria is becoming a global threat which has led to great concern in therapeutic approach to combat these pathogens[1]. Some of the commonly isolated pathogenic strains like, *Escherichia coli* and *Staphylococcus aureus*, have been found to possess certain enzymes like β-lactamases, which can delimit the potency of certain antibiotics[2]. In order to overcome this situation, alternative approaches are being looked on and nanoparticles have been identified as a strong candidate to combat these types of microorganisms[3,4]. AgNPs and CuNPs exhibit potent antimicrobial activity under all conditions[5,6]. Comparative analysis of their antimicrobial activity has revealed a strong variation due to many factors. Because of their capacity to damage bacterial cell membranes, produce reactive oxygen species ROS, and obstruct vital enzymatic processes, AgNPs are well known for their potent and broad-spectrum antibacterial activity[7,8]. AgNPs and CuNPs offer distinct advantages over other nanoparticles like zinc oxide (ZnO_2), titanium dioxide (TiO_2), and iron oxide (Fe_2O_2), particularly in antimicrobial applications unlike ZnO_2 and TiO_2, which require UV light for activation[9]. The broad-spectrum antimicrobial efficacy and stability of AgNP and CuNP makes them highly suitable for diverse biomedical and environmental applications[10].

Previous studies have focused largely on the general antibacterial effects of metal nanoparticles without investigating the precise growth dynamics of bacterial pathogens when exposed to these antimicrobials[11,12]. The present research introduces a novel framework for evaluating antibacterial treatments by quantifying the specific growth rate (µ) and doubling time (T_d) of bacteria exposed to biosynthesized nanoparticles. By incorporating growth rate kinetics and doubling time calculations, this study provides new insights into the efficacy of these nanoparticles, particularly in comparison to standard treatments. This approach allows for a rigorous assessment of the antibacterial activity and enhances our understanding of how these nanoparticles can effectively combat multidrug-resistant bacteria.

Materials and Methods

Biosynthesis of AgNP and CuNP

Biosynthesis of AgNP and CuNP was carried out using the extracellular extract of *Klebsiella pneumoniae*-NSB2 strain (Genbank Accession No.

*Correspondence:
E-mail: kunalmadhav.dntl.gn@its.edu.in

OP596438), which was isolated from Neem tree rhizosphere soil sample by using a previously mentioned protocol with slight modification[13]. The bacterial strain was freshly grown in 50 mL of Brain Heart Infusion Broth for 48 h at 37°C followed by centrifugation at 10,000 rpm for 15 min to obtain the extracellular extract. For the biosynthesis of AgNP, 90 mL of 1 mM $AgNO_3$ was mixed with 10 mL of the extracellular extract, followed by incubation in dark conditions at 25°C for 72 h[14]. Similarly, CuNP was prepared using same extracellular extract and mixed with 1 mM of $Cu(NO_3)_2.3H_2O$ followed by incubation at 25°C for 72 h under dark conditions. The presumed nanoparticles thus obtained was purified by centrifuging the nanoparticle solution at 15,000 rpm for 10 min. The supernatant was then discarded and the pellet was washed three times with sterile double distilled water followed by final wash using absolute ethanol to remove the impurities. The pellet was dried in oven at 100°C and grounded to powdered form next day. The powdered AgNPs and CuNPs were further characterized on the basis of their characteristic properties and antibacterial activities.

Characterization of Ag and CuNP

The synthesized AgNP and CuNP were analysed for their Surface Plasmon Response using a UV-Visible Spectrophotometer (Shimadzu UV-1800) with a scanning range of 200-800 nm[15]. Their crystallinity was examined via X-ray diffraction (XRD) technique using a Pan-Analytical X'Pert PRO diffractometer (Netherlands), with Cu-Kα radiation (λ = 1.54059 Å) across an angular range of 20-80˚ at 40 kV and 30 mA[16]. Additionally, the size and surface morphology of the nanoparticles were assessed by depositing the sonicated nanoparticles on copper grids, which were then dried and examined under a Transmission Electron Microscope (JEOL-JEM-1400) at an accelerating voltage of 120 kV[17].

Bacterial Culture

Bacterial cultures *E. coli* (MTCC 443) and *S. aureus* (MTCC 96) were procured from Microbial Type Culture Collection (MTCC), Chandigarh (India) for the assessment. The freeze-dried cultures thus procured were aseptically added to sterile tube of Brain Heart Infusion Broth (BHIB) and incubated for 24 h at 37°C[18]. The growth thus obtained was then streaked on sterile Trypticase Soy Agar (TSA) plates, followed by incubation for 24 h at 37°C.

Antibacterial activity

For the assessment of antibacterial activity, the Selected pathogens bacterial isolates were inoculated in sterile Brain Heart Infusion Broth (BHIB) and incubated at 37°C for 18 hours. The bacterial growth obtained next day was inoculated in freshly prepared sterile BHIB and the cell density was adjusted as per the MacFarland Standard followed by incubation at 37°C for 4 hours. With the help of sterile swab, the bacterial culture was swabbed on sterile Muller Hinton Agar (MHA) plates followed by incubation at room temperature (25 °C) for 10 minutes [19,20]. Sterile borers were used to create 6 mm diameter wells in the plates, into which 50 µL of AgNP and CuNP were introduced. Negative controls consisted of 1 mM solutions of silver nitrate ($AgNO_3$) and copper nitrate trihydrate [$Cu(NO_3)_2 \cdot 3H_2O$], while Streptomycin sulphate (50 µg/mL) was employed as a positive control.

Minimum Inhibitory Concentration (MIC) and Minimum Bactericidal Concentration (MBC) evaluation:

Broth dilution method was used for the assessment of the minimal inhibitory concentration of AgNPs and CuNPs. Based on the concentration of nanoparticles used in the previous studies, 10-50 µg/mL of AgNP and CuNP were added to the freshly inoculated Muller Hinton Broth (MHB) comprising of *E coli* and *S. aureus* respectively, followed by incubation at 37°C for 24 h. The MIC values were determined based on the presence or absence of the turbidity. From the MIC tubes, 100 µL of the sample was inoculated on the sterile nutrient agar plates, followed by incubation at 37°C for 24 h. The concentration of the nanoparticles which displayed no growth of bacteria was designated as its MBC[21].

Growth kinetics assessment:

For the evaluation of antibacterial activity and its impact on the growth curve, the concentration of 10-50 µg/mL of AgNP and CuNP were incorporated into broth cultures containing selected pathogens. These cultures were incubated at 37°C, with OD readings taken at 600 nm every 30 min over a 24 h time period. Negative controls consisted of 1 mM solutions of $AgNO_3$) and $Cu(NO_3)_2 \bullet 3H_2O$, while Streptomycin sulphate (50 µg/mL) was used as a positive control. Based on the result obtained, the specific growth rate 'µ' was calculated by using the following equation:

$$\mu = \frac{\ln(Nt) - \ln(N0)}{t}$$

[Where, μ is specific growth rate constant, ln(Nt) is the natural log value of the population of bacteria at a given time interval while ln (N0) is natural log value of the population of bacteria at the initial time interval and *t* is the final time duration]

Further, the effect of AgNP and CuNP was assessed by evaluating the doubling time 'T_d' of the bacteria by using the following equation:

$$Td = \frac{\ln(2)}{\mu}$$

[Where, μ is specific growth rate constant and ln(2) is the natural log value of the doubling bacterial population]

Statistical analysis

All results were analysed using GraphPad Prism 8.0 and R for statistical assessment. Data are expressed as mean values ± standard deviation from at least three independent experiments (n=3). Statistical significance was determined using ANOVA followed by Tukey's multiple comparisons test, with a significance threshold of $P < 0.05$.

Results

Characterization of AgNPs and CuNPs

After incubating the extracellular lysate of the bacterium with 1 mM silver nitrate ($AgNO_3$) and copper nitrate trihydrate [$Cu(NO_3)_2 \cdot 3H_2O$], the colour changes of the pale-yellow solution to amber brown indicating the formation of silver nanoparticles (AgNPs), while the colour change from pale green to brown indicated the formation of copper nanoparticles (CuNPs), as shown in Fig. 1A&B. Absorption peak was found to be around 422 nm and 419 nm for AgNP and CuNP respectively as shown in Fig. 2A&B. The presence of these peaks can be correlated with the bio-reduction of the AgNO3 and Cu(NO3)2 salts which assisted in converting their ionic states and the mediated synthesis of nanoparticles. Crystalline structure of AgNP and CuNP revealed various peaks on XRD analysis, confirming the crystallized property of nanoparticles as shown in Fig. 3A&B. In case of AgNPs the peaks were seen at the 2θ angels of 38.22°, 45.46°, 56.38^0 and 75.28° while for CuNPs the peaks were observed at 31.55°, 34.25°, 43.19°, 50.29°, 54.13° and 74.03°. The peaks thus obtained at these angels were found to have face centre cubic pattern in accordance with the 2θ angels of JCPDS file no. 00-004-0834 for Copper and 00-001-1164 for Silver. Topological and shape assessment by TEM revealed

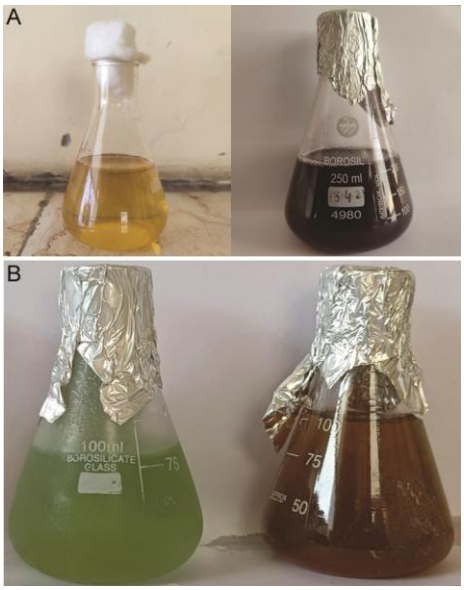

Fig. 1 — (A) Synthesis of AgNPs: Visible change of the colour of 1mM AgNO3 solution from pale yellow to brown after the addition of extracellular extract of K. pneumoniae-NSB2 strain followed by incubation; (B) Synthesis of CuNPs: Visible change of the colour of 1mM Copper Nitrate trihydrate [$Cu(NO_3)_2 \cdot 3H_2O$] Solution from pale green to dark brown, indicating the formation of Copper Nanoparticles (CuNP).

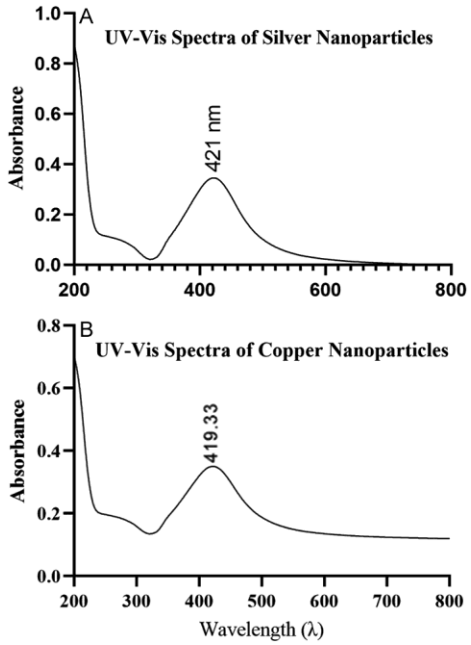

Fig. 2 — (A) UV-vis spectra of silver nanoparticles (AgNPs): Peak of the biosynthesized AgNP was observed at 421 nm; (B) UV-vis spectra of copper nanoparticles (CuNPs): Peak of the biosynthesized CuNP was observed at 419.33 nm.

the circular morphology of AgNPs and CuNPs as shown in Fig. 4A&B. By using Image J software, the mean diameter of the AgNPs and CuNPs were

calculated and it was observed that the size of AgNP was 29.3 nm and CuNP was 31.5 nm.

Antibacterial activity

Well diffusion experiment was performed to measure the antibacterial activity and observed that AgNPs demonstrated high antibacterial activity against all the test pathogens compared to CuNPs. The zone of inhibition displayed by these nanoparticles against the bacterial pathogens is shown in Table 1 and Fig. 5. In the present study, CuNPs displayed a zone of inhibition against *S. aureus* that was closer to that of the antibiotic. Comparative analysis of the antibacterial effects of AgNP, CuNP and a positive control (Streptomycin sulphate) against *E. coli* and *S. aureus* revealed significant findings. For *E. coli*, the AgNPs demonstrated a markedly higher antibacterial effect compared to CuNPs, with a mean difference of 11.19 mm (P = 0.0101), indicating a statistically significant difference. Similarly, when comparing AgNPs to the streptomycin sulphate, the mean difference was 8.050 mm (P = 0.0023), also showing a significant enhancement in antibacterial activity. However, the comparison between CuNPs and the streptomycin sulphate did not yield a statistically significant difference, with a mean difference of -3.140 mm (P = 0.0832), suggesting that CuNPs and the streptomycin sulphate have comparable effects on *E. coli*. For *S. aureus*, the AgNPs again showed superior antibacterial activity compared to CuNPs, with a mean difference of 11.35 mm (P = 0.0051), indicating a significant difference. The comparison between AgNPs and streptomycin sulphate also revealed a significant difference, with a mean difference of 10.20 mm (P = 0.0033). The comparison between CuNPs and the positive control showed a statistically significant difference, with a mean difference of -1.154 mm (P = 0.0350), indicating that CuNPs are slightly less effective than the positive control against *S. aureus* as shown in Fig. 6. These results highlight the potential of AgNPs as a more potent antibacterial agent in comparison to CuNPs and standard treatments. The statistical analysis further supports the significant

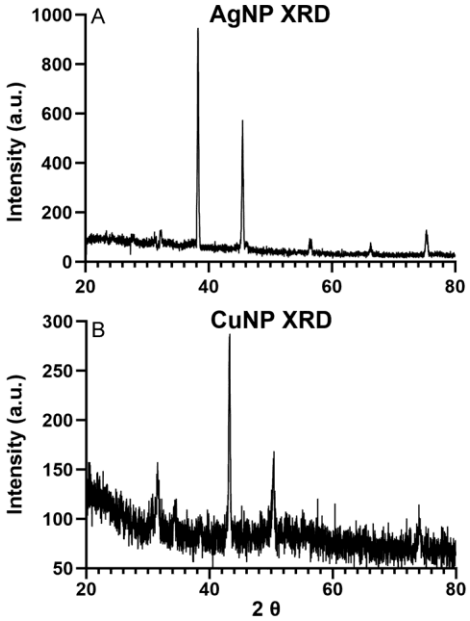

Fig. 3 — (A) XRD Peaks of AgNPs were seen at the 2θ angels of 38.22°, 45.46°, 56.38° and 75.28°; (B) XRD Peaks of CuNPs were seen at the 2θ angels of 31.55°, 34.25°, 43.19°, 50.29°, 54.13° and 74.03^0.

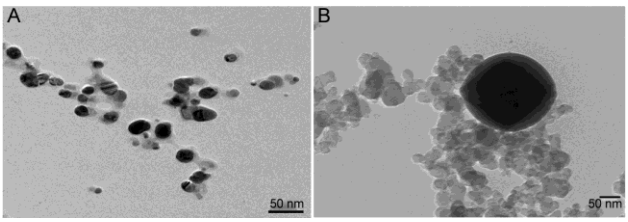

Fig. 4 — (A) TEM image of AgNPs and (B) TEM image of CuNPs.

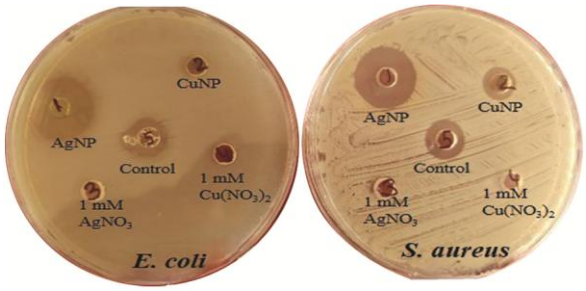

Fig. 5 — Antibacterial activity of AgNPs and CuNPs against *E. coli* and *S. aureus*

Table 1 — Antibacterial activity of AgNP and CuNP against *E. coli* and *S. aureus*

Test samples	*E. coli* (Mean ± SD) Zone of inhibition (mm)	*S. aureus* (Mean ± SD) Zone of inhibition (mm)
AgNP	23.26 ± 0.51	21.34 ± 0.32
CuNP	11.91 ± 0.29	11.79 ± 0.84
Positive control	13.06 ± 0.07	14.93 ± 0.26

differences in antibacterial activity, emphasizing the superior effectiveness of AgNPs.

MIC and MBC evaluation

MIC and MBC values of AgNP and CuNP against two bacterial strains, *E. coli* and *S. aureus*, were evaluated. The results revealed that MIC of AgNP against both *E. coli* and *S. aureus* was found to be 30 µg/mL, indicating that at this concentration, the growth of both bacterial strains was successfully inhibited. However, for CuNP, MIC was slightly higher for *E. coli* at 40 µg/mL, suggesting that a higher concentration of CuNP is required to inhibit the growth of this gram-negative bacterium compared to AgNP. It was also observed that the MIC for *S. aureus* was 30 µg/mL which was identical to that of AgNP, indicating that both types of nanoparticles were equally effective against this gram-positive bacterium at that concentration. Further analysis of MBC values, which represent the lowest concentration required to kill the bacteria, showed that AgNP had an MBC of 40 µg/mL for both *E. coli* and *S. aureus*. This implies that while 30 µg/mL of AgNP was sufficient to inhibit bacterial growth, a slightly higher concentration was needed to completely eradicate the bacteria. For CuNP, the MBC was also 40 µg/mL for both bacterial strains, reflecting a similar bactericidal potency as AgNP, despite the slight variation in MIC values for *E. coli*. These findings highlight that AgNP and CuNP exhibit strong antibacterial effects against both gram-negative (*E. coli*) and gram-positive (*S. aureus*) bacteria, with AgNP showing slightly superior inhibitory effects at lower concentrations for *E. coli*.

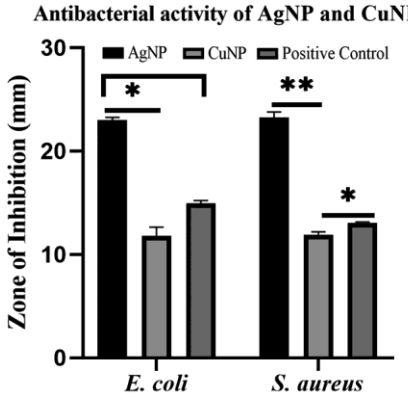

Fig. 6 — Two-way ANOVA based assessment of antibacterial activity of AgNPs and CuNPs against *E. coli* and *S. aureus*. **= *P value* < 0.005, * = *P value* < 0.05.

Growth kinetics assessment

The antibacterial activity of AgNP and CuNP was assessed by calculating the turbidimetric evaluation of the bacterial culture grown in the presence and absence of these nanoparticles. The reading thus obtained was calculated using the equations for the estimation of specific growth rate 'µ' and doubling time 'T_d' and summarized in Table 2 & Table 3 , respectively. It can be deduced from the table that both *E. coli* and *S. aureus* exhibits slower growth due to which the T_d increases along with the increase in nanoparticle's concentration in the beginning and at the highest concentration of 50 µg/mL, no growth was displayed by either of the bacteria. Secondly, it was also observed that at lower concentrations, AgNPs suppress the growth of both *E. coli* as well as *S. aureus* initially as compared to CuNP. But as the concentration of both AgNP and CuNP increases above 30 µg/mL, a strong decline in µ and T_d and of *E. coli* and *S. aureus* is noticed as shown in Fig. 7A-D. In both cases, it is clearly seen that when these pathogens are exposed to AgNP and CuNP, their µ decreases while the T_d increases.

Table 2 — Effect of AgNP & CuNP on specific growth rate(µ) of *E. coli* & *S. aureus*

Concentration (µg/mL)	AgNPs						CuNPs					
	E. coli			*S. aureus*			*E. coli*			*S. aureus*		
10	0.2594	0.2642	0.2637	0.3181	0.3177	0.3221	0.233	0.2278	0.2331	0.1749	0.1747	0.1749
20	0.2387	0.2396	0.2412	0.2177	0.2044	0.2058	0.1743	0.1732	0.1742	0.2007	0.2015	0.2004
30	0.1227	0.123	0.121	0.159	0.152	0.1564	0.1706	0.1704	0.1708	0.1659	0.174	0.1741
40	0.1227	0.1231	0.1238	0.1469	0.1518	0.153	0.142	0.1247	0.1421	0.1661	0.1682	0.1689
50	0.1003	0.1	0.101	0.1199	0.102	0.1031	0.1199	0.1191	0.12	0.1003	0.1	0.1009
PC	0.1003	0.1002	0.1002	0.1395	0.141	0.1462	0.1003	0.1002	0.1002	0.1395	0.141	0.1462
#NC	0.6842	0.6794	0.6742	0.5314	0.5718	0.5416	-	-	-	-	-	-
*NC	-	-	-	-	-	-	0.7421	0.7394	0.7468	0.6125	0.6122	0.6097

[Positive control(PC) = Streptomycin sulphate (50 µg/mL), #Negative Control(#NC) = 1mM $Ag(NO)_3$, *Negative Control (*NC) = 1mM $[Cu(NO_3)_2 \cdot 3H_2O]$]

Table 3 — Effect of AgNP & CuNP on doubling time(T_d) of *E. coli* & *S. aureus*

Concentration	AgNPs						CuNPs					
(µg/mL)	*E. coli*			*S. aureus*			*E. coli*			*S. aureus*		
10	267	266	268	220	218	218	298	300	303	420	423	419
20	290	291	288	321	318	320	398	400	403	349	347	345
30	565	562	571	440	436	438	406	410	412	439	438	436
40	565	562	563	483	479	481	488	490	495	452	453	448
50	691	689	694	621	606	610	606	612	615	691	695	691
PC	691	692	696	529	521	523	691	693	693	526	523	521
#NC	119	120	117	182	174	178	-	-	-	-	-	-
*NC	-	-	-	-	-	-	119	122	126	180	176	174

[Positive control(PC) = Streptomycin sulphate (50 µg/mL), #Negative Control(#NC) = 1mM $Ag(NO)_3$, *Negative Control (*NC) = 1mM $[Cu(NO_3)_2 \cdot 3H_2O]$

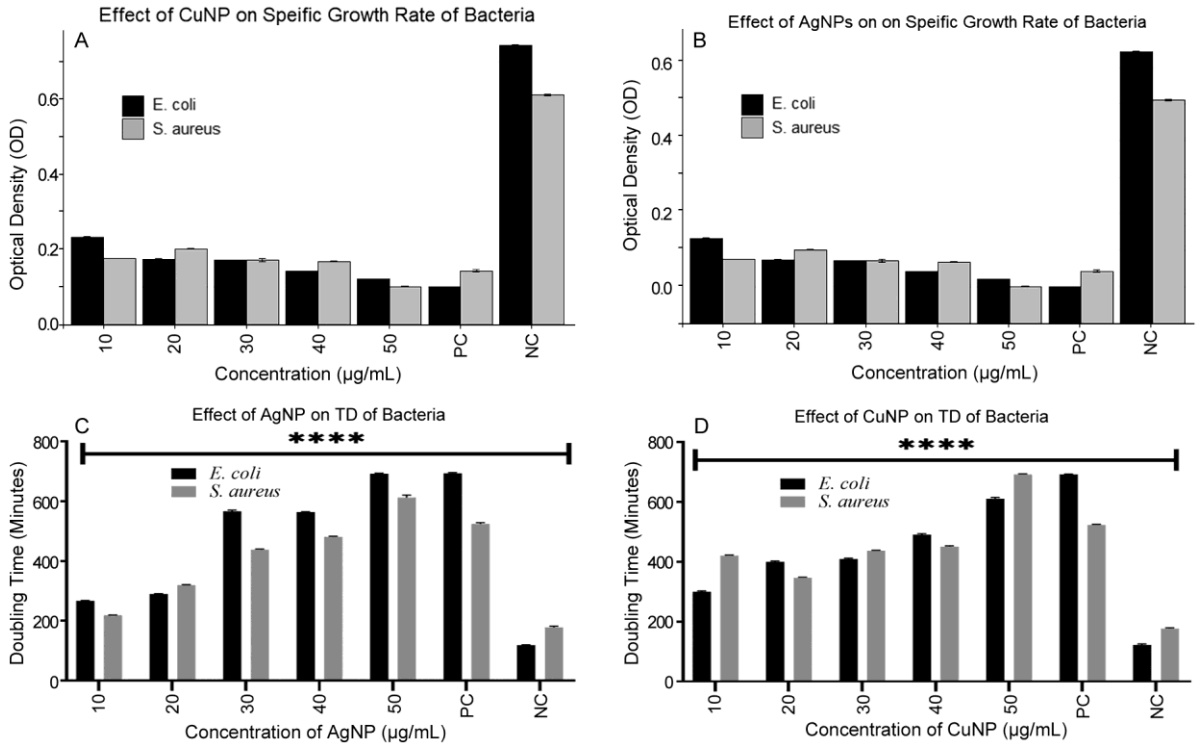

Fig. 7 — Effect of nanoparticles on specific growth rate of bacteria (A) CuNPs; (B) AgNPs and effect of nanoparticles on doubling time (T_d) of bacteria (C) AgNPs; (D) CuNPs.

Discussion

Quantifying the impact of nanoparticles on bacterial growth rates can help researchers to develop a more effective treatment for antibiotic-resistant infections while utilizing a mathematical model that computes and correlates bacterial proliferation could be a key parameter in evaluating their potency[22,23]. While silver and copper nanoparticles have been widely studied. The biosynthesis of nanoparticles using *K. pneumoniae*-NSB2 strain and their impact on bacterial growth dynamics, particular growth rate and doubling time, is not well explored. Applying a mathematical model that correlates the rapid proliferation of bacteria and nanoparticle inhibition offers a clear understanding of how silver and copper nanoparticles can be utilized as alternatives to antibiotics in combating drug-resistant bacterial strains[11,24]. One of the essential parameters for the confirmation of the nanoparticle synthesis is the change of colour which is indicated by the shift in Surface Plasmon Resonance (SPR)[25,26]. This change of SPR is due to the conversion of the metallic ions of Ag^+ to Ag^0 and Cu^+ to Cu^0 state, which is then measured using a UV-Vis spectrophotometer[27,28].

Similar results pertaining to the colour change during the AgNP and CuNP synthesis has been reported in previous studies[29]. The antibacterial activity of nanoparticles is mediated by several mechanisms, including the generation of ROS, disruption of the bacterial cell membrane, and interaction with bacterial DNA and proteins[30]. The release of silver ions (Ag^+) of AgNPs play a crucial role in its antimicrobial activity by binding to the bacterial cell membrane and proteins, disrupting essential cellular functions such as respiration and DNA replication[31]. The smaller size of AgNPs enhances their ability to penetrate bacterial cells, which is another reason for their superior antibacterial activity compared to CuNPs[21,32]. The ability of AgNPs to target multiple cellular pathways makes them highly effective antimicrobial agents and reduces the likelihood of bacteria developing resistance. CuNPs, while slightly less effective than AgNPs, also exhibit strong antibacterial properties[33]. The antimicrobial activity of CuNPs is primarily due to the release of copper ions (Cu^{2+}), which can disrupt bacterial cell membranes and generate ROS[34]. The generation of ROS leads to oxidative damage to bacterial proteins, lipids, and DNA, ultimately resulting in cell death. However, the larger size of CuNPs compared to AgNPs may limit their ability to penetrate bacterial cells, which could explain their relatively lower antibacterial activity[35,36]. Previous research has described the role of silver to bind chemical entities of bacteria like Thiol groups of the respiratory enzymes, thus inhibiting the respiratory process and hence eliminating[37,38]. Similarly, in copper nanoparticles studies have mentioned that they can generate ROS as well as replace the cofactors in metalloproteins in the microorganisms[39]. It has been reported that due to their complex cell wall, the gram positive bacteria are often found to have higher tolerance against the antimicrobial agents including antibiotics[40] and nanoparticles[41], which in the present study was not evident. This may be due to the interaction of the nanoparticles on the cell of the gram-positive and gram-negative bacteria which have rich content of peptidoglycan and lipo-polysaccharides in their cell wall and also the presence of carboxyl, phosphates and other amino acid groups that imparts a negative charge on the cell wall[42]. Studies have shown that AgNPs have the potential to interact with these negative charges, which leads to the binding of the positively charged nanoparticles, leading to the penetration and elimination of bacteria[43].

The determination of MIC and MBC of AgNP and CuNP was performed using a turbidimetric method, which measures bacterial growth by assessing the turbidity or cloudiness of a bacterial culture. In this study, the MIC of AgNP was 30 μg/mL for both *E. coli* and *S. aureus*, while the MIC for CuNP was 40 μg/mL for *E. coli* and 30 μg/mL for *S. aureus*. These results indicate that AgNP is slightly more effective than CuNP in inhibiting bacterial growth, particularly against *E. coli*. This difference in efficacy can be attributed to the smaller size of AgNPs, which allows them to penetrate bacterial cell membranes more easily. The MBC for both AgNP and CuNP was 40 μg/mL for both bacterial strains, indicating that while AgNP may inhibit bacterial growth more effectively at lower concentrations, both nanoparticles are equally capable of killing bacteria at higher concentrations. The fact that both nanoparticles exhibited bactericidal properties is significant because it suggests that they could be used to prevent bacterial growth and eliminate existing bacterial populations.

Despite significant progress in the study of metal nanoparticles, a critical research gap remains in exploring alternative biosynthesis methods and quantifying their antibacterial effects using bacterial growth kinetics[44]. The application of mathematical models to calculate μ and T_d offers a deeper understanding of bacterial inhibition kinetics[45]. No bacterial growth was observed at higher concentrations (50 μg/mL), suggesting that both AgNP and CuNP can completely eradicate bacterial populations at sufficient doses. This finding is particularly relevant for medical applications, where preventing bacterial regrowth is essential for preventing infections. The extended T_d observed in the presence of both nanoparticles further supports their ability to inhibit bacterial reproduction and suggests that they could be used as effective antimicrobial agents in a variety of settings[46]. Both nanoparticles were found to significantly reduce μ of both bacterial strains, indicating that they effectively inhibit bacterial proliferation. The reduction in bacterial growth rate is an important indicator of the nanoparticles' ability to prevent bacterial colonization and biofilm formation, which are major challenges in the treatment of bacterial infections[47]. Further research on the safety and optimization of nanoparticle usage in clinical settings is necessary to advance these promising findings. Additionally, the data suggests that CuNPs

may be more effective during the early growth phase of these pathogens, potentially leading to early cessation of bacterial growth, a hypothesis that requires further exploration.

Conclusion

Outcomes of the study conclude that AgNPs had a significantly greater zone of inhibition than CuNPs against both bacterial strains, confirming their superior efficacy. Growth kinetics analysis revealed that AgNPs and CuNPs reduced bacterial growth rates (μ) and increased doubling times (T_d), with AgNPs exhibiting a more pronounced effect. CuNPs displayed moderate antibacterial properties, their activity remained lower than AgNPs and the positive control (streptomycin sulfate). These findings highlight the potential of biosynthesized AgNPs as an effective antibacterial agent and provide valuable insights for optimizing nanoparticle-based antimicrobial strategies.

Acknowledgements

The authors would like to acknowledge IIT Delhi and AIIMS for providing the facility of XRD, Transmission Electron Microscopy and UV-Visible Spectrophotometer, respectively and Dr. Sachit Anand Arora (Principal, I.T.S Dental College, Greater Noida), Dr. Nitika Anand (HOD-Microbiology, I.T.S Dental College, Greater Noida) & Mr. Bhairav Pandey for the institutional, departmental and laboratory support respectively.

Conflict of interest

The authors have no conflict of interest to declare.

References

1 Poletajew S, Pawlik K, Bonder-Nowicka A, Pakuszewski A, Nyk Ł & Kryst P. Multi-drug resistant bacteria as aetiological factors of infections in a tertiary multidisciplinary hospital in poland. *Antibiotics*. 2021;10(10):1–10.

2 Jain N, Jansone I, Obidenova T, Simanis R, Meisters J, Straupmane D & Reinis A. Antimicrobial resistance in nosocomial isolates of gram-negative bacteria: Public health implications in the latvian context. *Antibiotics*. 2021;10(7):1–19.

3 Song X, Liu P, Liu X, Wang Y, Wei H, Zhang J, Yu L, Yan X & He Z. Dealing with MDR bacteria and biofilm in the post-antibiotic era: Application of antimicrobial peptides-based nano-formulation. *Mater Sci Eng C* [Internet]. 2021;128(July):1–23. Available from: https://doi.org/10.1016/j.msec.2021.112318

4 Murugan M, Rani KRB, Wins JA, Ramachandran G, Guo F, Mothana RA, Noman OM, Nasr FA & Siddiqi MZ. Green synthesized ZnO NPs as effective bacterial inhibitor against isolated MDRs and biofilm producing bacteria isolated from urinary tract infections. *J King Saud Univ - Sci* [Internet]. 2022;34(1):1–10. Available from: https://doi.org/10.1016/j.jksus.2021.101737

5 Ermini ML & Voliani V. Antimicrobial Nano-Agents: The Copper Age. *ACS Nano*. 2021;15(4):6008–29.

6 Dove AS, Dzurny DI, Dees WR, Qin N, Nunez Rodriguez CC, Alt LA, Ellward GL, Best JA, Rudawski NG, Fujii K & Czyż DM. Silver nanoparticles enhance the efficacy of aminoglycosides against antibiotic-resistant bacteria. *Front Microbiol*. 2023;13(January).

7 Keshari AK, Srivastava A, Chowdhury S & Srivastava R. Antioxidant and antibacterial property of biosynthesised silver nanoparticles. *Nanomedicine Res J*. 2021;6(1):17–27.

8 Novelles M del CT, Brown TSP, Feliciano DN, Travieso AG & Hernandez IR. Silver nanoparticles as proapoptotic drugs: pharmacological basis in non-metastatic skin melanoma. *Pharm Pharmacol Int J*. 2022;10(3):66–74.

9 Benčina M, Iglič A, Mozetič M & Junkar I. Crystallized tio2 nanosurfaces in biomedical applications. *Nanomaterials*. 2020;10(6).

10 Hemalatha M, Hilli JS, Chandrashekhar SS, Vijayakumar AG, Reddy UG & Tippannavar PS. Application of green synthesized Ag and Cu nanoparticles for the control of bruchids and their impact on seed quality and yield in greengram. *Heliyon*. 2024;10(11).

11 Pedreira A, Vázquez JA & García MR. Kinetics of Bacterial Adaptation, Growth, and Death at Didecyldimethylammonium Chloride sub-MIC Concentrations. *Front Microbiol*. 2022;13(April):1–11.

12 Adawiyah R, Rohim A, Muhamad W, Ahmad AW, Ismail NH, Muna F, Ghazali M & Alam MK. Modeling the Growth of Bacteria Streptococcus sobrinus Using Exponential Regression. *Pesqui Bras Odontopediatria Clin Integr*. 2020;(20:e5380):1–7.

13 Kumar V, Parida SN, Dhar S, Bisai K, Sarkar DJ, Panda SP & Das BK. Biogenic synthesis of silver nanoparticle by Cytobacillus firmus isolated from the river sediment with potential antimicrobial properties against Edwardsiella tarda. *Front Microbiol*. 2024;15(August):1–12.

14 Madhav K & Pandita A. Biosynthesis of Silver Nanoparticles from Klebsiella pneumoniae and analysis of its Haemato-Toxic and Antibacterial Properties . 2023;10:2366–78.

15 Kareem SO, Adeleye TM & Ojo RO. Effects of pH, temperature and agitation on the biosynthesis of iron nanoparticles produced by Trichoderma species. *IOP Conf Ser Mater Sci Eng*. 2020;805(1).

16 Ullah Z, Gul F, Iqbal J, Abbasi BA, Kanwal S & Chalgham W. Biogenic Synthesis of Multifunctional Silver Oxide Nanoparticles (Ag 2 ONPs) Using Parieteria alsinaefolia Delile Aqueous Extract and Assessment of Their Diverse Biological Applications. *Microorganisms*. 2023;11(1069):1–19.

17 John MS, Nagoth JA, Ramasamy KP, Mancini A, Giuli G, Miceli C & Pucciarelli S. Synthesis of Bioactive Silver Nanoparticles Using New Bacterial Strains from an Antarctic Consortium. *Mar Drugs*. 2022;20(9):1–13.

18 Knobloch JKM, Horstkotte MA, Rohde H & Mack D. Evaluation of different detection methods of biofilm formation in Staphylococcus aureus. *Med Microbiol Immunol*. 2002;191(2):101–6.

19 Addis T, Mekonnen Y, Ayenew Z, Fentaw S & Biazin H. Bacterial uropathogens and burden of antimicrobial resistance pattern in urine specimens referred to Ethiopian Public Health Institute. *PLoS One* [Internet]. 2021;16(11

November):1–14. Available from: http://dx.doi.org/10.1371/journal.pone.0259602

20 Munusamy T & Shanmugam R. Green Synthesis of Copper Oxide Nanoparticles Synthesized by Terminalia chebula Dried Fruit Extract: Characterization and Antibacterial Action. *Cureus*. 2023;15(12).

21 Wypij M, Jędrzejewski T, Trzcińska-Wencel J, Ostrowski M, Rai M & Golińska P. Green Synthesized Silver Nanoparticles: Antibacterial and Anticancer Activities, Biocompatibility, and Analyses of Surface-Attached Proteins. *Front Microbiol*. 2021;12(April).

22 Ghosh S, Ahmad R, Zeyaullah M & Khare SK. Microbial Nano-Factories: Synthesis and Biomedical Applications. *Front Chem.* 2021;9(April):1–19.

23 Krishnamurthi VR, Niyonshuti II, Chen J & Wang Y. A new analysis method for evaluating bacterial growth with microplate readers. *PLoS One* [Internet]. 2021;16(1 January):1–19. Available from: http://dx.doi.org/10.1371/journal.pone.0245205

24 Grasso A Lo, Fort A, Mahdizadeh FF & Magnani A. Generalized logistic model of bacterial growth. Math Comput Model *Dyn Syst*. 2023;29(1):169–85.

25 Singla S, Jana A, Thakur R, Kumari C, Goyal S & Pradhan J. Green synthesis of silver nanoparticles using Oxalis griffithii extract and assessing their antimicrobial activity. *OpenNano* [Internet]. 2022;7(May):100047. Available from: https://doi.org/10.1016/j.onano.2022.100047

26 Abdollahzadeh MR, Meshkatalsadat MH & Pouramiri B. Synthesis and Characterization of Copper Nanoparticles utilising Pomegranate Peel Extract and Its Antibacterial activity. *Int Res J Mod Eng Technol Sci*. 2023;10(1):43–52.

27 Oves M, Rauf MA & Qari HA. Therapeutic Applications of Biogenic Silver Nanomaterial Synthesized from the Paper Flower of Bougainvillea glabra (Miami, Pink). *Nanomaterials*. 2023;13(3).

28 Elshaer S & Shaaban MI. Antibiofilm activity of biosynthesized silver and copper nanoparticles using Streptomyces S29. *AMB Express* [Internet]. 2023;13(1). Available from: https://doi.org/10.1186/s13568-023-01647-3

29 Naseer QA, Xue X, Wang X, Dang S, Din SU, Kalsoom & Jamil J. Synthesis of silver nanoparticles using lactobacillus bulgaricus and assessment of their antibacterial potential. *Brazilian J Biol.* 2022;82:1–8.

30 More PR, Pandit S, Filippis A De, Franci G, Mijakovic I & Galdiero M. Silver Nanoparticles: Bactericidal and Mechanistic Approach against Drug Resistant Pathogens. *Microorganisms*. 2023;11(2).

31 Fouda A, Awad MA, Al-Faifi ZE, Gad ME, Al-Khalaf AA, Yahya R & Hamza MF. Aspergillus flavus-Mediated Green Synthesis of Silver Nanoparticles and Evaluation of Their Antibacterial, Anti-Candida, Acaricides, and Photocatalytic Activities. *Catalysts.* 2022;12(5):1–19.

32 Gupta D, Yadav P, Garg D & Gupta TK. Pathways of nanotoxicity: Modes of detection, impact, and challenges. *Front Mater Sci.* 2021;15(4):512–42.

33 Vijayakumar G, Kim HJ & Rangarajulu SK. In Vitro Antibacterial and Wound Healing Activities Evoked by Silver Nanoparticles Synthesized through Probiotic Bacteria. *Antibiotics*. 2023;12(1):1–21.

34 Shehabeldine AM, Amin BH, Hagras FA, Ramadan AA, Kamel MR, Ahmed MA, Atia KH & Salem SS. Potential Antimicrobial and Antibiofilm Properties of Copper Oxide Nanoparticles: Time-Kill Kinetic Essay and Ultrastructure of Pathogenic Bacterial Cells. Appl Biochem Biotechnol [Internet]. 2023;195(1):467–85. Available from: https://doi.org/10.1007/s12010-022-04120-2

35 Munuswamy T, Rajeshkumar S, Al-Ghanim KA, Nicoletti M, Sachivkina N & Govindarajan M. Terminalia chebula - Assisted Silver Nanoparticles: Biological Potential, Synthesis, Characterization, and Ecotoxicity. *Biomedicines*. 2023;11(1472):1–18.

36 Ali AY, Alani AAK, Ahmed BO & Hamid LL. Effect of biosynthesized silver nanoparticle size on antibacterial and anti-biofilm activity against pathogenic multi-drug resistant bacteria. *OpenNano*. 2024;20(July).

37 Illanes Tormena RP, Medeiros Salviano Santos MK, Oliveira da Silva A, Félix FM, Chaker JA, Freire DO, Rodrigues da Silva IC, Moya SE & Sousa MH. Enhancing the antimicrobial activity of silver nanoparticles against pathogenic bacteria by using Pelargonium sidoides DC extract in microwave assisted green synthesis. *RSC Adv*. 2024;14(30):22035–43.

38 Sadeghi E, Taghavi R, Hasanzadeh A & Rostamnia S. Bactericidal behavior of silver nanoparticle decorated nano-sized magnetic hydroxyapatite. *Nanoscale Adv.* 2024;6166–72.

39 Ma X, Zhou S, Xu X & Du Q. Copper-containing nanoparticles: Mechanism of antimicrobial effect and application in dentistry-a narrative review. *Front Surg.* 2022;(August):1–21.

40 Siriphap A, Kitti T, Khuekankaew A, Boonlao C, Thephinlap C, Thepmalee C, Suwannasom N & Khoothiam K. High prevalence of extended-spectrum beta-lactamase-producing Escherichia coli and Klebsiella pneumoniae isolates: A 5-year retrospective study at a Tertiary Hospital in Northern Thailand. *Front Cell Infect Microbiol.* 2022;12(August) :4–11.

41 Kamat S & Kumari M. Emergence of microbial resistance against nanoparticles: Mechanisms and strategies. Front *Microbiol.* 2023;14.

42 Aguilar-Garay R, Lara-Ortiz LF, Campos-López M, Gonzalez-Rodriguez DE, Gamboa-Lugo MM, Mendoza-Pérez JA, Anzueto-Ríos Á & Nicolás-Álvarez DE. A Comprehensive Review of Silver and Gold Nanoparticles as Effective Antibacterial Agents. *Pharmaceuticals.* 2024;17(9):1134.

43 Girma A. Antibacterial Capabilities of Metallic Nanoparticles and Influencing Factors. *Nano Sel.* 2024;1–16.

44 Chatterjee N, Pal S, Chakraborty A & Dhar P. Bacteria against bacteria: Green silver nanoparticle fabrication, antioxidant, anti-biofilm and antibacterial activities. *Indian J Chem Technol.* 2024;31(3):411–24.

45 Rodrigues AS, Batista JGS, Rodrigues MÁV, Thipe VC, Minarini LAR, Lopes PS & Lugão AB. Advances in silver nanoparticles: a comprehensive review on their potential as antimicrobial agents and their mechanisms of action elucidated by proteomics. *Front Microbiol.* 2024;15(July).

46 Niu B & Zhang G. Effects of Different Nanoparticles on Microbes. *Microorganisms.* 2023;11(3):1–16.

47 Aflakian F, Mirzavi F, Aiyelabegan HT, Soleimani A, Gholizadeh Navashenaq J, Karimi-Sani I, Rafati Zomorodi A & Vakili-Ghartavol R. Nanoparticles-based therapeutics for the management of bacterial infections: A special emphasis on FDA approved products and clinical trials. *Eur J Pharm Sci.* 2023;188(March).